Flavonoid from *Hedera helix* fruits: A promising new natural sensitizer for DSSCs

Makbule Erdogdu [a,*], Abdullah Atilgan [b], Yusuf Erdogdu [c], Abdullah Yildiz [b]

[a] *Department of Landscape Architects, Faculty of Agriculture, Kırşehir Ahi Evran University, Kırşehir 40100, Turkey*
[b] *Department of Energy Systems Engineering, Faculty of Engineering and Natural Sciences, Ankara Yildirim Beyazıt University, Ankara 06010, Turkey*
[c] *Department of Physics, Faculty of Science, Gazi University, 06500 Teknikokullar, Ankara, Turkey*

ARTICLE INFO

ABSTRACT

Owing to their lower cost, simplicity of manufacture, environmental friendliness, and accessibility of raw materials, natural dyes emerge as the most viable substitute for dye-sensitized solar cells (DSSCs). However, the photovoltaic performance of DSSCs based on natural dyes stays behind that of their metal-based counterparts. This can be partially overcome when appropriate chemical additives are present in the redox electrolyte employed in DSSCs based on natural dyes. To determine the ideal additives for DSSCs based on natural dye extracted from Hedera helix fruits, including flavonoid pigments, we thoroughly compare the actions of 1-butyl-3-methylimidazolium iodide, guanidinium thiocyanate, and *tert*-butylpyridine additives in ionic liquid-based redox electrolytes. These additives suppress undesirable charge recombination and parasitic resistance effects, achieving a more significant enhancement of open-circuit voltage (Voc) of 130 mV and fill factor (FF) of 30 % compared to their counterparts. Utilizing prepared electrolyte solutions in DSSCs also presents an outstanding increase in the efficiency of the devices, from 0.75 % to 1.17 % (~56 % improvement), which outperforms other natural dye sources containing flavonoid pigments as well. The experimental findings provided in this study demonstrate that the development of electrolytes tailored for natural dyes can lead to greater power conversion efficiency.

1. Introduction

Dye-sensitized solar cells (DSSCs) possess the capacity to transform light into electrical energy through the stimulation of light sensitization on a semiconductor material characterized by a wide energy band [1–5]. DSSCs have garnered significant interest owing to their comparatively reduced production expenses. Due to their straightforward manufacturing procedure, DSSCs may be produced under normal conditions at ambient temperature, providing a cost-benefit of roughly 33 % compared to conventional silicon-based solar cells.

The sensitizer choice significantly influences the DSSC's efficiency [6–9]. Considerable study endeavors have been devoted to advancing sensitizers for DSSCs. The absorption spectrum of the photosensitizer dye in visible light is crucial in improving the efficiency of DSSCs. This specific characteristic facilitates the provision of electrons to the conduction band of titanium dioxide (TiO_2) and enhances the efficiency of the electron transfer process [10–13].

Three distinct categories of dye sensitizers are metal complex, metal-free, and natural [14]. Natural sensitizers are readily accessible from fruits, flowers, leaves, and other plant components [15]. Numerous metal complex sensitizers, including ruthenium [16], osmium [17], platinum [18], copper [19], and iridium [20], have been investigated for DSSC.

The heightened photo-conversion efficiency of Ruthenium (II) metal-based compounds makes them commonly used as dyes in DSSCs [21,22]. Considerable investigation has been undertaken on the polypyridyl complex of the metallic element ruthenium, which has been widely utilized in several fields, encompassing natural, organic, and inorganic sensitizers. This is primarily attributed to this complex's exceptional stability and unique redox properties. Nevertheless, using dyes based on Ruthenium is associated with notable disadvantages, such as their prohibitively high expense and the requirement for complex synthesis methods that include substantial levels of toxicity and present environmental hazards.

Research and testing have been done on natural dyes to find cheaper alternatives to the rare and expensive ruthenium compounds. In
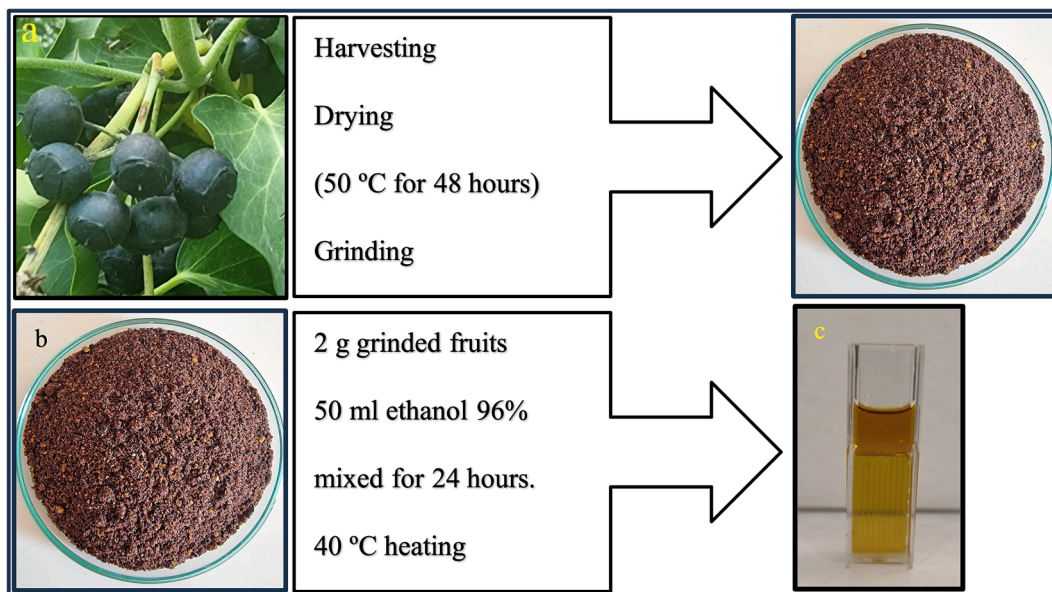

Fig. 1. A) *Hedera Helix* plant and fruits, b) the grinded fruits, and c) the extracted dye solutions.
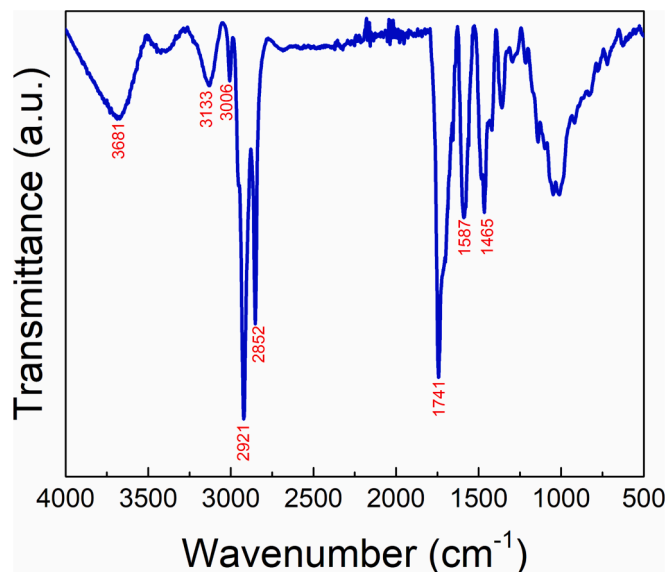
Fig. 2. The FT-IR spectra of the dye solution from extracted *Hedera helix* fruits.

Fig. 3. The FT-IR spectra of the spectra of the dye loaded and unloaded TiO2.

comparison to ruthenium polypyridyl complexes, natural dyes are significantly more affordable and straightforward to produce. Their low binding energies with titanium dioxide (TiO_2) and constrained ability to absorb and transmit charges across the visible spectrum typically hinder their photovoltaic performance in DSSCs [23]. Given the intriguing potential of cells formed from natural dyes, it is imperative to intensify research efforts to augment their functioning. A wide range of environmentally friendly natural dyes is readily available. Utilizing mordant and auxiliary substances significantly enhances the dye's rigidity and the cell's durability. The manufacturing expenses are relatively inexpensive. Several important factors led to using cells made from natural pigments in this study [24].

Similar to the synthesis process of Ruthenium-based dyes, producing metal-free synthetic organic sensitizers also necessitates an intricate synthesis methodology. However, it is imperative to note that natural colors can be readily derived from diverse sources, such as flowers, fruits, leaves, stems, roots, seeds, and so on. The comparative efficiency
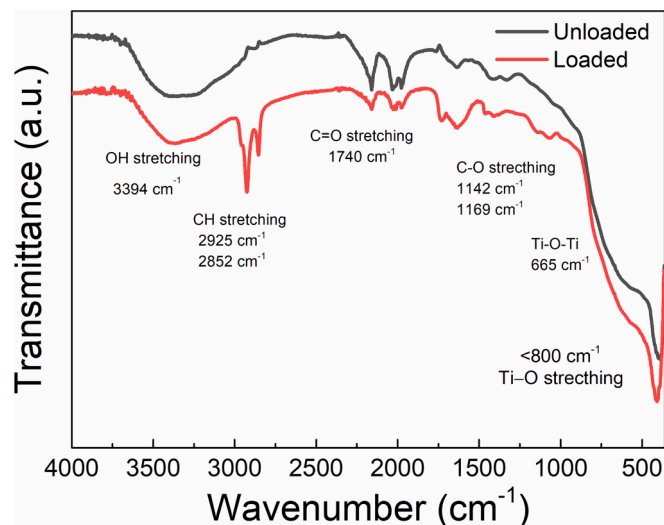
of DSSCs employing natural sensitizers is substantially inferior to that of DSSCs utilizing ruthenium-based dyes and metal-free synthesized organic dyes. Natural dyes do not necessitate intricate synthesis and extraction methodologies, unlike ruthenium-based dyes or metal-free organic synthetic dyes. Natural dyes possess considerable potential due to their cost-effectiveness, biodegradability, non-toxicity, and positive environmental impact. In contemporary times, many natural organic pigments, such as anthocyanin, luteolin, tannin, chlorophyll, and beta-carotene, have been effectively employed as light-absorbing agents in DSSCs [25–31].

The triiodide/iodide redox pair is most frequently used in high-performance DSSCs [1–5]. The corrosion of silver-based current collectors and the partial absorption of visible light at about 430 nm by the triiodide species are two downsides of this redox pair despite its efficiency [32]. As a result, researching additives is crucial.

Various pigments and dyes obtained from different plant species have demonstrated varying levels of efficiency in converting solar energy into electrical energy. This efficiency is influenced by the chemical composition of the dyes and the degree to which they are absorbed onto
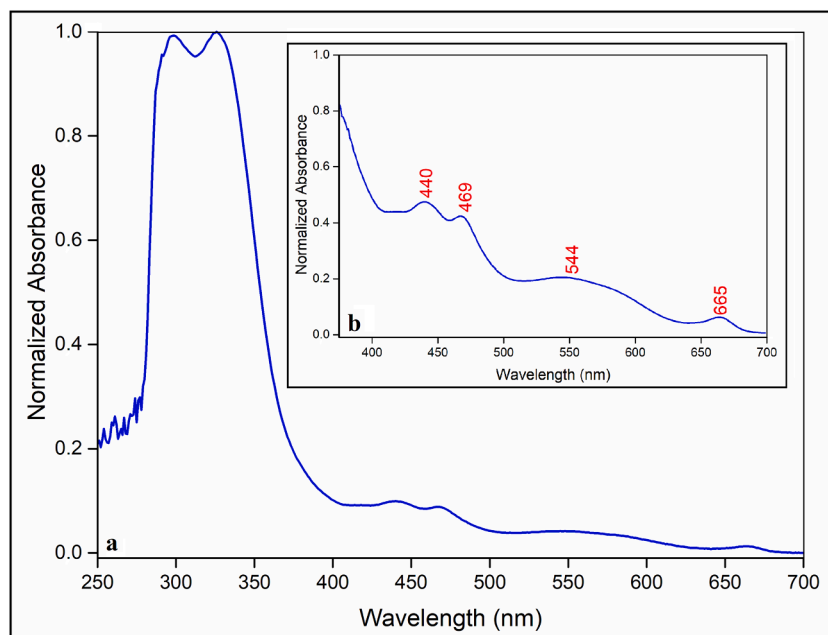
Fig. 4. The UV–Vis spectra of the dilute (a) and concentrate(b) dye solution from extracted *Hedera helix* fruits.
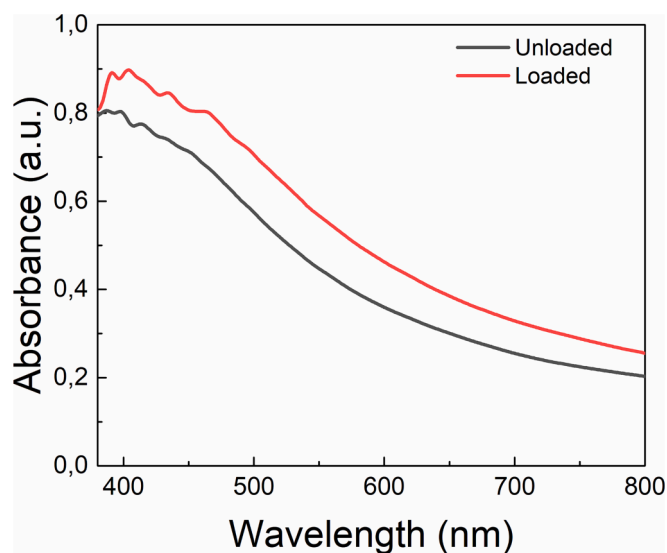

Fig. 5. The UV–Vis absorption spectra of the dye loaded and unloaded TiO2 electrodes

Fig. 6. The J-V and P-V curves of the device based on various electrolytes.

Table 1
The photovoltaic performance of the devices based on different electrolytes was tested under standard AM 1.5 irradiation (100 mWcm^{-2}).

DYE	J_{SC} (mA/ cm^2)	V_{OC} (V)	FF	η (%)	P_{max} (mW)
EL1	2.35	0.65	0.77	1.17	1.18
	2.30 ± 0.04	0.65 ± 0.01	0.77 ± 0.01	1.17 ± 0.01<	1.17 ± 0.01<
EL2	3.04	0.52	0.47	0.75	0.76
	3.01 ± 0.06	0.52 ± 0.01	0.47 ± 0.01	0.75 ± 0.03	0.75 ± 0.01

* Average values and standard deviations of five devices.

the mesoporous TiO$_2$ surface. The range of numbers provided is between 6 and 9. The extract derived from the fruits of *Hedera helix* contains flavonoid pigments, which exhibit distinct light-harvesting capabilities due to their UV–vis absorption properties. This research investigates the characteristics and effectiveness of natural dyes derived from *Hedera helix* fruit as a sensitizer in DSSCs using various electrolytes, marking the first instance of such exploration.

2. Experimental

2.1. Plant material

The climbing, evergreen genus Hedera L. belongs to the Araliaceae family and is found throughout Asia, Europe, Macaronesia, and North Africa [33]. One of our native species, Hedera helix L., is a woody vine
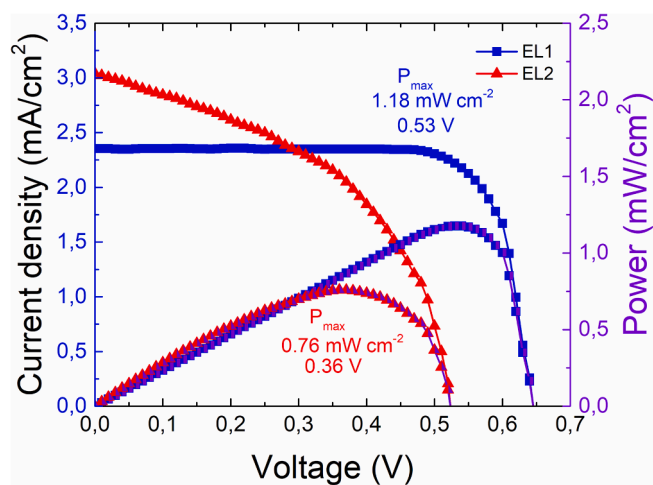
that creeps on the ground or climbs up a vertical structure. It can grow up to 30 m tall and have stems up to 20 cm in diameter [34]. Young shoots and inflorescences have stellate hairs covering them. The leaves are glabrous, narrowly elliptic to suborbicular-cordate, mostly whole, and measure 5–8 × 5–10 cm on flowering shoots; they are palmately
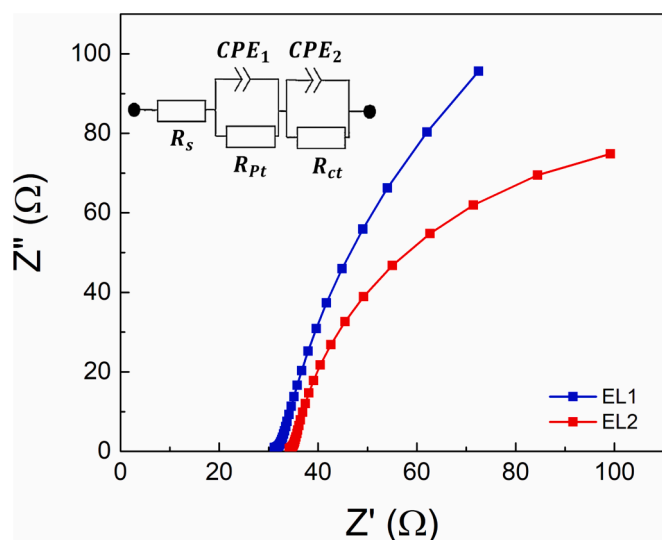
Fig. 7. EIS measurements of the devices using various electrolytes.

Table 2
Parameters estimated from EIS measurements of the devices based on different electrolytes.

Electrolyte	R_s (Ω)	R_{ct} (Ω)	R_{rec} (Ω)	η_c (%)
EL1	25.84	7.51	413.2	0.98
EL2	18.54	18.8	169.5	0.90

3–5-lobed and measure (2–) 4–8 × 2–6 cm on sterile shoots [35]. The petals of the corolla are greenish, the teeth of the calyx are typically poorly formed, and the flowers are generally dioecious. The mature fruits are bluish-black berries 8–10 mm in diameter and have two to five seeds. The fruits are spherical. Fruits ripen from March to April (June), and flowers bloom between September and October [34].

2.2. Preparation of natural dye sensitizers

Hedera helix fruit extract was the natural dye utilized in this study as a light sensitizer to produce DSSCs. The plant materials (Hedera helix fruits) were gathered in Kirsehir, Turkey. Then, a voucher specimen was placed in the Kirsehir Ahi Evran University herbarium. For around 48 h, the fruits were dried at 50 °C. The dried samples were then grinded into powder form (Fig. 1). The grinded fruits (2 g) were extracted in a mixer for 24 h with 50 ml of 96 % ethanol. The extraction procedure also included a 40 °C heating approach. The extract was filtrated the next day. Until analysis, all extracts were kept at + 4 °C in a light-protected environment.

2.3. Preparation of Dye-Sensitized solar cells

A layer of Mesoporous TiO$_2$, with a thickness of approximately ~ 13

μm and composed of 20 nm particles (specifically, Degussa P25, Aeroxide TiO$_2$ P 25, Evonik), was successfully deposited over FTO conducting glass. The FTO conducting glass exhibited a surface resistance of around ~ 7 Ω/sq and a visual transmittance range of 80–82 %. The FTO conducting glass used in this study was obtained from Sigma Aldrich. The counter electrode utilized in the experiment was a thermally platinized FTO conducting glass. To sensitize the electrode, it was subjected to a solution containing 2 g of natural dye extract dissolved in 50 ml of ethyl alcohol. This exposure occurred at room temperature and in a dark environment for 24 h. The active area of the photoanodes is measured to be 0.27 cm^2. The research team investigated the photovoltaic capabilities of the integrated sourcemeter (Keithley, 2400) test station while subjecting it to illumination from a sun simulator (ABET, LS-150). The measurements of the current–voltage curves were conducted at AM 1.5 (1 Sun) circumstances. The electrochemical impedance spectroscopy measurements were performed at open circuit voltage using a Gamry test station (model 1000E).

The composition of the electrolytes:

The electrolyte EL1 is composed of a mixture of volatile solvents and exhibits redox behavior involving the I$^-$/I$_3^-$ redox couple. It consists of 0.6 M 1-butyl-3-methylimidazolium iodide (BMII), 0.1 M lithium iodide, 0.05 M iodine, 0.05 M guanidinium thiocyanate, and 0.5 M *tert*-butylpyridine, all dissolved in a mixture of valeronitrile and acetonitrile in a volumetric ratio of 15:85.

EL2 is an ionic liquid consisting of a mixture of 0.6 M 1-butyl-3-methylimidazolium iodide, 0.1 M lithium iodide, 0.01 M iodine, and 0.1 M *tert*-butylpyridine dissolved in 3-methoxypropionitrile.

3. Results and discussion

3.1. Chemical composition

More data on the chemical makeup of ivy fruits and flowers needs to be published. According to Parvu et al., p-coumaric acid, ferulic acid, rutoside, quercetol, and kaempferol were detected in the extract of Hedera helix fruits in the non-hydrolyzed sample. In contrast, p-coumaric acid, ferulic acid, sinapic acid, quercetol, and kaempferol were identified in the hydrolyzed sample [36]. The ripe fruits of the Hedera helix extract were found to contain the maximum concentration of phenolic and flavonoid components, according to another study by Pop et al. [37]. The ethanolic extract, which includes flavonoids for the natural dye, was produced from the fruits of *Hedera helix*. Hydroxyl (–OH) and carboxyl (–COOH) groups are essential for DSSC study in natural dyes. By way of these functional groups, the interaction required to transfer electrons from the dye molecule to the TiO$_2$ is shown. To help with the electron transfer mechanism, the carbonyl (–COOH) and hydroxyl (–OH) groups on flavonoid molecules can interact with TiO$_2$.

3.2. Fourier transform infrared spectroscopy

The natural dye FT-IR transmittance curve of the natural dye is shown in Fig. 2. These spectra were measured between 4000 and 400 cm^{-1} using a Thermo Scientific Nicolet 6700. While intermolecular hydrogen bonding can lower the O-H stretching wavenumber to the

Table 3
Comparison of the results for various DSSCs based on natural dyes consisting of natural pigment of flavonoid in the literature.

Source for dye	Electrolyte	J_{SC} (mA/cm^2)	V_{OC} (V)	FF	η (%)	Reference
C. Fistula flower	LiI, I$_2$, ACN	0.54	0.51	0.65	0.21	[47]
C. Odontophyllum	TBAI, I$_2$, ACN, EC	3.54	0.42	0.59	0.68	[48]
Cosmos sulphureus	Iodolyte AN-50	1.04	0.45	0.61	0.54	[49]
Kigelia Africana	LiI, I$_2$, TBP	5	0.48	0.36	0.87	[50]
P. betle	–	6.35	0.33	0.52	1.09	[51]
Nasturtium	–	0.72	0.55	0.70	0.28	[52]
Rubiaceae	TBAI, I$_2$, ACN, EC	3.38	0.49	0.58	0.95	[53]
Hedera helix	EL1	2.35	0.65	0.77	1.17	This study

3550–3200 cm^{-1} range, the free or unbound hydroxyl group absorbs significantly in the 3700–3584 cm-1 range [38]. The O-H functional group can be observed at 3681 cm^{-1} on the FT-IR pattern for the *Hedera helix* dye. The stretching vibration mode of the carbonyl group (CO) is represented by the peak in the area between 1780 and 1700 cm^{-1} [39]. The CO group is present in the FT-IR spectra of the dye at 1741 cm^{-1}. The dye's carbonyl group can establish bonds with semiconductor oxides, which makes it easier for the dye to inject electrons into the TiO$_2$ surface.

The Fourier-transform infrared (FT-IR) spectra of photoanodes loaded with dye and those without dye were obtained using a JASCO FT/IR-6X spectrophotometer equipped with attenuated total reflection (ATR) units. The spectra were recorded in the wavenumber range of 4000 to 350 cm^{-1}, as depicted in Fig. 3. Upon comparing the Fourier Transform Infrared (FTIR) spectra of photoanodes that are unloaded and loaded with dye, it has been observed that a broad peak is present at 3335 cm^{-1}, which corresponds to the stretching modes of hydroxyl (O–H) in the unloaded photoanode. However, this peak undergoes a blue shift in the photoanode adsorbed with natural dye and is observed at 3394 cm^{-1} [25–27]. However, it is possible to attribute the existence of a widened peak at around 1068 cm^{-1} to the strong stretching vibrations of Ti-O interactions. This suggests that dye molecules have been successfully adsorbed onto the surface of TiO$_2$ [10]. The peaks detected at 1137 cm^{-1} can be ascribed to the stretching modes of the –C–O–C– moiety.

In contrast, the peak at 1734 cm^{-1} can be assigned to the stretching vibration mode of the carbonyl group, as reported in previous studies [27,31,40]. The electron injection process from the dye into TiO$_2$ is assisted by the presence of a carbonyl group, which can form bonds with semiconductor oxides. Therefore, the efficiency of DSSCs is enhanced [25].

3.3. Absorption spectroscopy

The UV–Vis absorption spectra offer significant insights into multiple factors, including the absorption of the solar spectrum by the photoanode and the absorption transition between the ground and excited states of the dye molecule. Flavonoid molecules possess carbonyl and hydroxyl groups in their chemical composition, which enable their interaction with the TiO$_2$ layer and augment the efficiency of power conversion. The absorption spectra of the extracted dye between 250 and 700 nm were measured using the Thermo Scientific GENESYS 10S UV–Vis spectrophotometer, as shown in Fig. 4. The dye demonstrates maximum absorbances within the 400 to 700 nm wavelength range, with specific peak absorbances at 440, 469, 544, and 665 nm (Fig. 5).

The Shimadzu UV-1700 UV spectrophotometer was utilized for conducting UV spectroscopic analysis. Fig. 4 displays the spectra of photoanodes loaded with dye and those that are unloaded. The photoanode exhibited enhanced performance across the whole range following dye loading, with the most notable enhancement observed within the 450–600 nm region.

3.4. Photovoltaic measurements

The performance of the dye as a sensitizer in DSSCs based on various electrolytes under typical AM 1.5 irradiation (100 mWcm^{-2}) was examined under ambient conditions. In Fig. 4, the devices' photocurrent density–voltage (J-V) and power-voltage (P-V) curves are displayed. Open-circuit voltage (V_{oc}), short-circuit current density (J_{sc}), fill factor (*FF*), and photovoltaic efficiency (η) are the photovoltaic parameters of the devices shown in Fig. 6 and are summarized in Table 1.

The device based on EL1 exhibits an excellent efficiency of 1.17 % with the J_{sc} of 2.35 mA/cm^2, the V_{oc} of 0.65 V, and the *FF* of 0.77. Once EL2 is included in the device, both V_{oc} (0.52 V) and *FF* (0.47) decrease dramatically. The substitution of EL1 with EL2 increases the Jsc value from 2.35 mA/cm^2 to 3.04 mA/cm^2. However, despite this gain, the overall efficiency of the device remains considerably lower (0.75 %) compared to the device utilizing EL1.

The primary distinction between the two electrolytes lies in the varying quantities of iodine and *tert*-butylpyridine, including guanidinium thiocyanate in el1, and the dissimilar solvents employed. The acetonitrile-valeronitrile solvent pair has superior power conversion efficiency to the more thermally stable 3-methoxyethanol solvent despite the latter's higher boiling point. This discrepancy can be attributed to the enhanced conductivity of the former solvent pair. The work conducted by Shah et al. (41) demonstrated that the addition of GuSCN to the electrolyte solution led to improved performance of DSSCs. The observed enhancement can be ascribed to the adsorption of guanidinium cations onto the oxide semiconductor material. The incorporation of GuSCN into the electrolyte has the ability to induce a change in the conduction band towards a higher positive potential. The occurrence of this event will cause an increase in the rate at which electrons are injected, thus resulting in a rise in the value of Jsc. The increase in Voc can be ascribed to the obstructive influence of adsorbed ions on the recombination sites on the surface of the oxide semiconductor [41]. Furthermore, it is postulated that the modifications in the concentrations of iodine and *tert*-butylpyridine may have resulted in an adverse shift in the redox potential of the electrolyte. This elucidates the inverse relationship between the short-circuit current (Jsc) and the open-circuit voltage (Voc), wherein Jsc decreases while Voc increases.

Compared to EL2, a higher value of Voc for EL1 might be associated with the negative shift of Fermi energy (upward band edge shift) [42,43], suppression of recombination losses [30], and the lower redox potential of E1 concerning E2 [44]. Compared to EL2, a more excellent value of FF for EL1 might be accompanied by decreasing parasitic resistance effects [45]. These findings may be rationalized by the fact that replacing EL1 with EL2 leads to enhanced efficiency for the dye extracted from Hedera helix fruits, and E2 can be a promising choice for dyes containing flavonoids. Further studies are in progress to clarify the underlying mechanisms involving the utilization of the electrolytes in DSSCs. Summarizing the presented results, the anodes consisting of EL1 are the most promising for DSSC preparation.

Electrochemical impedance spectroscopy (EIS), employing the cells built with two distinct electrolytes, was used to understand better the charge transfer properties of the devices (Fig. 7). With the aid of the appropriate equivalent circuit shown in Fig. 7, the resulting EIS spectra were fitted [45]. The series resistance (R_s) is represented by the intercept on the real axis in the Nyquist plots. The semicircles are brought on by the recombination resistance (R_{rec}) at the electrode/electrolyte/dye interface and the charge transfer resistance (R_{ct}) at the electrode/electrolyte interface of the counter electrode. The EL1-based device exhibits relatively lower R_{ct} and higher R_{rec}. From the measured impedance data, the charge collecting efficiency (η_c) value of the devices can be estimated using the equation $\eta_c = [1 + (R_{ct}/R_{rec})]^{-1}$ [46]. The higher η_c value found for the EL1-based device compared to that of the EL2-based device demonstrates better charge transfer and collection, leading to an increment in the performance of the DSSC (Table 2).

Table 3 compares the DSSCs in this study and other reported DSSCs, whose structures include the natural pigment of flavonoids. From this comparison, it can be concluded that our device has better *FF* and V_{oc} values than the other reported devices, translating to an encouraging performance.

4. Conclusions

In brief, this study presents the novel utilization of cost-effective natural dye derived from *Hedera helix* fruits as a sensitizer in DSSCs with various electrolytes. The improved efficacy of the devices when utilizing an appropriate electrolyte can be attributed to the combined impact of mitigating undesired charge recombination and minimizing parasitic resistance effects. However, further improvement in the

selection of materials may contribute to the development of improved electrolytes, thereby enhancing the performance of the device. Further investigation is needed to understand the fundamental physical mechanisms that underlie the performance of electrolyte-dependent devices. However, we anticipate that such studies will offer valuable insights into the potential of natural dyes for application in DSSCs.

CRediT authorship contribution statement

Makbule Erdogdu: Writing – review & editing, Resources, Investigation, Conceptualization. **Abdullah Atilgan:** Visualization, Formal analysis, Data curation. **Yusuf Erdogdu:** Writing – review & editing, Resources, Investigation, Conceptualization. **Abdullah Yildiz:** Visualization, Formal analysis, Data curation.

Declaration of Competing Interest

The authors declare that they have no known competing financial interests or personal relationships that could have appeared to influence the work reported in this paper.

Data availability

Data will be made available on request.

References

[1] M. Grätzel, Dye-sensitized solar cells, J. Photochem. Photobiol. C: Photochem. Rev. 4 (2) (2003) 145–153, https://doi.org/10.1016/S1389-5567(03)00026-1.

[2] A. Yildiz, T. Chouki, A. Atli, M. Harb, S.W. Verbruggen, R. Ninakanti, S. Emin, Efficient iron phosphide catalyst as a counter electrode in dye-sensitized solar cells, ACS Appl. Energy Mater. 4 (1010) (2021) 10618–10626, https://doi.org/10.1021/acsaem.1c01628.

[3] A. Atilgan, A. Yildiz, Ni-doped TiO2/TiO2 homojunction photoanodes for efficient dye-sensitized solar cells, Int. J. Energy Res. 46 (10) (2022) 14558–14569, https://doi.org/10.1002/er.8175.

[4] A. Atli, A. Atilgan, Yildiz, "Multi-layered TiO2 photoanodes from different precursors of nanocrystals for dye-sensitized solar cells", Sol. Energy 173 (2018) 752–758, https://doi.org/10.1016/j.solener.2018.08.027.

[5] A. Atli, A. Yildiz, Opaque Pt counter electrodes for dye-sensitized solar cells, Int. J. Energy Res. 46 (5) (2022) 6543–6552, https://doi.org/10.1002/er.7590.

[6] K. Tennakone, G.R.R.A. Kumara, A.R. Kumarasinghe, P.M. Sirimanne, K.G. U. Wijayantha, Efficient photosensitization of nanocrystalline TiO2 films by tannins and related phenolic substances, J. Photochem. Photobiol. A Chem. 94 (2–3) (1996) 217–220, https://doi.org/10.1016/1010-6030(95)04222-9.

[7] A. Atli, A. Atilgan, C. Altinkaya, K. Ozel, A. Yildiz, St. Lucie cherry, yellow jasmine, and madder berries as novel natural sensitizers for dye-sensitized solar cells, Int. J. Energy Res. 43 (8) (2019) 3914–3922, https://doi.org/10.1002/er.4538.

[8] Y. Kocak, A. Atli, A. Atilgan, A. Yildiz, Extraction method dependent performance of bio-based dye-sensitized solar cells (DSSCs), Mater. Res. Express 6 (9) (2019), 095512, https://doi.org/10.1088/2053-1591/ab2ef7.

[9] Y. Kocak, A. Yildiz, Carminic acid extracted from cochineal insect as photosensitizer for dye-sensitized solar cells, Int. J. Energy Res. 45 (11) (2021) 16901–16907, https://doi.org/10.1002/er.6883.

[10] V. Yadav, C.M.S. Negi, D.K. Kumar, S.K. Gupta, Fabrication of eco-friendly, low-cost dye sensitized solar cells using harda fruit-based natural dye, Opt. Mater. 122 (2021), 111800, https://doi.org/10.1016/j.optmat.2021.111800.

[11] V. Yadav, S. Chaudhary, C.M.S. Negi, S.K. Gupta, Textile dyes as photo-sensitizer in the dye sensitized solar cells, Opt. Mater. 109 (2020), 110306, https://doi.org/10.1016/j.optmat.2020.110306.

[12] D. Kharkwal, N. Sharma, S.K. Gupta, C.M.S. Negi, Enhanced performance of dye-sensitized solar cells by co-sensitization of metal-complex and organic dye, Sol. Energy 230 (2021) 1133–1140, https://doi.org/10.1016/j.solener.2021.11.037.

[13] N. Akdogan, M. Alp, A. Atilgan, A. Disli, Y. Erdogdu, A. Yildiz, An AZO dye with nitril anchoring to dye-sensitized solar cell performance: A theoretical and experimental investigation, Mater. Lett. 351 (2023), 135075, https://doi.org/10.1016/j.matlet.2023.135075.

[14] A. Ashok, S.E. Mathew, S.B. Shivaram, S.A. Shankarappa, S.V. Nair, M. Shanmugam, Cost effective natural photo-sensitizer from upcycled jackfruit rags for dye sensitized solar cells, J. Sci.: Adv. Mater. Devices 3 (2) (2018) 213–220, https://doi.org/10.1016/j.jsamd.2018.04.006.

[15] P.G. Bomben, K.C. Robson, B.D. Koivisto, C.P. Berlinguette, Cyclometalated ruthenium chromophores for the dye-sensitized solar cell, Coord. Chem. Rev. 256 (15-16) (2012) 1438–1450, https://doi.org/10.1016/j.ccr.2012.02.005.

[16] V.V.W. Yam, V.K.M. Au, S.Y.L. Leung, Light-emitting self-assembled materials based on d8 and d10 transition metal complexes, Chem. Rev. 115 (15) (2015) 7589–7728, https://doi.org/10.1021/acs.chemrev.5b00074.

[17] H.V. Hierlinger, D.B. Flint, A.M. Cordes, E.A.G. Slawin, D. Jacquemin, E. Zysman-Colman, A panchromatic, near infrared Ir (III) emitter bearing a tripodal C^{NC} ligand as a dye for dye-sensitized solar cells, Polyhedron 140 (2018) 109–115, https://doi.org/10.1016/j.poly.2017.12.003.

[18] M.R. Elmorsy, R. Su, A.A. Fadda, H.A. Etman, E.H. Tawfik, A. El-Shafei, Effect of terthiophene spacer position in Ru (II) bipyridyl complexes on the photocurrent and photovoltage for high efficiency dye-sensitized solar cells, Dyes Pigm. 156 (2018) 348–356, https://doi.org/10.1016/j.dyepig.2018.04.005.

[19] M. Liang, J. Chen, Arylamine organic dyes for dye-sensitized solar cells, Chem. Soc. Rev. 42 (8) (2013) 3453–3488, https://doi.org/10.1039/C3CS35372A.

[20] M.R. Elmorsy, L. Lyu, R. Su, E. Abdel-Latif, S.A. Badawy, A. El-Shafei, A.A. Fadda, Co-sensitization of the HD-2 complex with low-cost cyanoacetanilides for highly efficient DSSCs, Photochem. Photobiol. Sci. 19 (2020) 281–288, https://doi.org/10.1039/c9 pp00381a.

[21] N. Sekar, V.Y. Gehlot, Metal complex dyes for dye-sensitized solar cells: Recent developments, Resonance 15 (9) (2010) 819–831.

[22] F. Kabir, S. Manir, M.M.H. Bhuiyan, S. Aftab, H. Ghanbari, A. Hasani, M.M. Adachi, Instability of dye-sensitized solar cells using natural dyes and approaches to improving stability–An overview, Sustainable Energy Technol. Assess. 52 (2022), 102196.

[23] P. Balraju, P. Suresh, M. Kumar, M.S. Roy, G.D. Sharma, Effect of counter electrode, thickness and sintering temperature of TiO2 electrode and TBP addition in electrolyte on photovoltaic performance of dye sensitized solar cell using pyronine G (PYR) dye, J. Photochem. Photobiol. A Chem. 206 (1) (2009) 53–63, https://doi.org/10.1016/j.jphotochem.2009.05.014.

[24] S. Vargas, I. Santamaria-Holek, R. Rodríguez, Photocurrent oscillations in natural dyes-based DSSCs with different mordant and assistants: Their role in oscillations and color stability, Mater. Chem. Phys. 286 (2022), 126163, https://doi.org/10.1016/j.matchemphys.2022.126163.

[25] B.C. Ferreira, D.M. Sampaio, R.S. Babu, A.L.F. De Barros, Influence of nanostructured TiO2 film thickness in dye-sensitized solar cells using naturally extracted dye from Thunbergia erecta flowers as a photosensitizer, Opt. Mater. 86 (2018) 239–246, https://doi.org/10.1016/j.optmat.2018.10.016.

[26] F.C. Ferreira, R.S. Babu, A.L.F. de Barros, S. Raja, L.R.B. da Conceição, L.H. C. Mattoso, Photoelectric performance evaluation of DSSCs using the dye extracted from different color petals of Leucanthemum vulgare flowers as novel sensitizers, Spectrochim. Acta A Mol. Biomol. Spectrosc. 233 (2020) 118198, https://doi.org/10.1016/j.saa.2020.118198.

[27] F.M.M. dos Santos, A.M.B. Leite, L.R.B. da Conceição, Y. Sasikumar, R. Atchudan, M.F. Pinto, A.L.F. de Barros, Effect of bandgap energies by various color petals of Gerbera jamesonii flower dyes as a photosensitizer on enhancing the efficiency of dye-sensitized solar cells, J. Mater. Sci. Mater. Electron. 33 (25) (2022) 20338–20352, https://doi.org/10.1007/s10854-022-08849-8.

[28] B.C. Ferreira, R.S. Babu, L.R.B. da Conceição, H.O. da Cunha, D.M. Sampaio, L. M. Samyn, A.L.F. de Barros, Performance evaluation of DSSCs using naturally extracted dyes from petals of Lantana repens and Solidago canadensis flowers as light-harvesting units, Ionics 28 (11) (2022) 5233–5242, https://doi.org/10.1007/s11581-022-04727-9.

[29] A.M.B. Leite, H.O. da Cunha, J.A.F.C.R. Rodrigues, R.S. Babu, A.L.F. de Barros, Construction and characterization of organic photovoltaic cells sensitized by Chrysanthemum based natural dye, Spectrochim. Acta A Mol. Biomol. Spectrosc. 284 (2023), 121780, https://doi.org/10.1016/j.saa.2022.121780.

[30] D.M. Sampaio, R.S. Babu, H.R.M. Costa, A.L.F. De Barros, Investigation of nanostructured TiO 2 thin film coatings for DSSCs application using natural dye extracted from jabuticaba fruit as photosensitizers, Ionics 25 (2019) 2893–2902, https://doi.org/10.1007/s11581-018-2753-6.

[31] L.R.B. da Conceição, A.L.F. de Barros, D.B. Haddad, R.S. Babu, Passiflora edulis and Cocos nucifera extracts as light-harvesters for efficient dye-sensitized solar cells, IEEE ANDESCON (2020).

[32] M. Wang, N. Chamberland, L. Breau, J.E. Moser, R. Humphry-Baker, B. Marsan, M. Grätzel, An organic redox electrolyte to rival triiodide/iodide in dye-sensitized solar cells, Nat. Chem. 2 (5) (2010) 385–389, https://doi.org/10.1038/nchem.610.

[33] E. Amini, F. Nasrollahi, A. Sattarian, M. Haji Moradkhani, M. Habibi, S. Boozarpour, Morphological and anatomical study of the genus *Hedera* in Iran, Rostaniha 20 (2) (2019) 144–157, https://doi.org/10.22092/BOTANY.2019.127705.1171.

[34] E. Vukičević, "Dekorativna dendrologija", Faculty of Forestry, University of Belgrade, Belgrade, 1996.

[35] P.H. Davis, Flora of Turkey and East Aegean Islands Vol. 4 (1972) 657.

[36] M. Parvu, L. Vlase, A.E. Parvu, O. Rosca-Casian, A.M. Gheldiu, O. Parvu, Phenolic compounds and antifungal activity of Hedera helix L. (Ivy) flowers and fruits, Notulae Botanicae Horti Agrobotanici Cluj-Napoca 43 (1) (2015) 53–58, https://doi.org/10.15835/NBHA4319644.

[37] C.E. Pop, M. Parvu, A.L. Arsene, A.E. Parvu, D.C. Vodnar, M. Tarcea, L. Vlase, Investigation of antioxidant and antimicrobial potential of some extracts from *Hedera helix* L, Farmacia 65 (2017) 624–629.

[38] Y. Erdogdu, Investigations of FT-IR, FT-Raman, FT-NMR spectra and quantum chemical computations of Esculetin molecule, Spectrochim. Acta A Mol. Biomol. Spectrosc. 106 (2013) 25–33, https://doi.org/10.1016/j.saa.2012.12.043.

[39] Y. Erdogdu, U.C. Baskose, S. Saglam, M. Erdogdu, H. Ogutcu, S. Özçelik, Structural, thermal, spectroscopic, electronic and biological activity properties of coumarin-153 dyes for DSSCs: A DFT benchmark study, J. Mol. Struct. 1221, 2020, pp.128873. https://doi.org/10.1016/j.molstruc.2020.128873.

[40] S. Jeyaram, T. Geethakrishnan, Vibrational spectroscopic, linear and nonlinear optical characteristics of anthocyanin extracted from blueberry, Results Optics 1 (2020), 100010, https://doi.org/10.1016/j.rio.2020.100010.

[41] S. Shah, N.N.S. Baharun, S.N.F. Yusuf, A.K. Arof, Efficiency enhancement of dye-sensitized solar cells (DSSCs) using copper nanopowder (CuNW) in TiO2 as photoanode, in: IOP Conference Series: Materials Science and Engineering, Vol. 515, IOP Publishing, 2019, April, p. 012002.

[42] Y. Wang, J. Lu, J. Yin, G. Lü, Y. Cui, S. Wang, Y. Sun, Influence of 4-tert-butyl-pyridine/guanidinium thiocyanate co-additives on band edge shift and recombination of dye-sensitized solar cells: experimental and theoretical aspects, Electrochim. Acta 185 (2015) 69–75, https://doi.org/10.1016/j.electacta.2015.10.103.

[43] M.J. Kim, N.G. Park, Urea as a long-term stable alternative to guanidium thiocyanate additive in dye-sensitized solar cell, Appl. Surf. Sci. 258 (22) (2012) 8915–8918, https://doi.org/10.1016/j.apsusc.2012.05.116.

[44] N.T. Salim, X. Yang, S. Zhang, J. Liu, A. Islam, L. Han, Shielding effects of additives in a cobalt (ii/iii) redox electrolyte: toward higher open-circuit photovoltages in dye-sensitized solar cells, J. Mater. Chem. A 2 (27) (2014) 10532–10539, https://doi.org/10.1039/C4TA01278J.

[45] A. Atli, I. Sutcu, Z.K. Yildiz, A. Yildiz, Optimizing Deposition Parameters of DSSCs Composed of Blue TiO2, IEEE J. Photovoltaics 11 (2021) 118–123, https://doi.org/10.1109/JPHOTOV.2020.3038602.

[46] M.R. Subramaniam, D. Kumaresan, S. Jothi, J.D. McGettrick, T.M. Watson, Reduced graphene oxide wrapped hierarchical TiO2 nanorod composites for improved charge collection efficiency and carrier lifetime in dye sensitized solar cells, Appl. Surf. Sci. 428 (2018) 439–447, https://doi.org/10.1016/j.apsusc.2017.09.142.

[47] I.C. Maurya, S. Singh, P. Srivastava, B. Maiti, L. Bahadur, Natural dye extract from Cassia fistula and its application in dye-sensitized solar cell: Experimental and density functional theory studies, Opt. Mater. 90 (2019) 273–280, https://doi.org/10.1016/j.optmat.2019.02.037.

[48] A. Lim, N.T.R.N. Kumara, A.L. Tan, A.H. Mirza, R.L.N. Chandrakanthi, M.I. Petra, P. Ekanayake, Potential natural sensitizers extracted from the skin of Canarium odontophyllum fruits for dye-sensitized solar cells, Spectrochim. Acta A Mol. Biomol. Spectrosc. 13 (2015) 596–602, https://doi.org/10.1016/j.saa.2014.11.102.

[49] M. Narayan, A. Raturi, Investigation of some common Fijian flower dyes as photosensi-tizers for dye sensitized solar cellsabstract, Appl. Solar Energy 47 (2011) 112–117, https://doi.org/10.3103/S0003701X11020149.

[50] S. Shalini, N. Prabavathy, R. Balasundaraprabhu, T.S. Kumar, D. Velauthapillai, P. Balraju, S. Prasanna, Studies on DSSC encompassing flower shaped assembly of Na-doped TiO2 nanorods sensitized with extract from petals of Kigelia Africana, Optik 155 (2018) 334–343, https://doi.org/10.1016/j.ijleo.2017.10.173.

[51] H. Jaafar, L. Magesvaran, Performance of P. betle extraction as sensitizer in dye-sensitized solar cells (DSSCs), in: IOP Conference Series: Earth and Environmental Science, vol. 596, IOP Publishing, 2020, p. 012027, https://doi.org/10.1088/1755-1315/596/1/012027.

[52] S. Singh, I.C. Maurya, S. Sharma, S.P.S. Kushwaha, P. Srivastava, L. Bahadur, Application of new natural dyes extracted from Nasturtium flowers (Tropaeolum majus) as photosensitizer in dye-sensitized solar cells, Optik 243 (2021), 167331, https://doi.org/10.1016/j.ijleo.2021.167331.

[53] N.T.R.N. Kumara, M. Petrović, D.S.U. Peiris, Y.A. Marie, C. Vijila, M.I. Petra, P. Ekanayake, Efficiency enhancement of Ixora floral dye sensitized solar cell by diminishing the pigments interactions, Sol. Energy 117 (2015) 36–45, https://doi.org/10.1016/j.solener.2015.04.019.